H2Open Journal

IWA PUBLISHING

H2Open Journal Vol 4 No 2, 656 doi: 10.2166/h2oj.2022.027

Jute (*Corchorus olitorius*) stick charcoal: a potential bioadsorbent for the removal of Cr(VI) from an aqueous solution

Samina Zaman[a,*], Pipasa Biswas[a], Rafiuz Zaman[b], Md. Shahnul Islam[a], Md. Nayeem Mehrab[a], Gopal Chandra Ghosh[a], Ahsan Habib[a] and Tapos Kumar Chakraborty[a]

[a] Department of Environmental Science and Technology, Jashore University of Science and Technology, Jashore, Bangladesh
[b] Department of Leather Engineering, Institute of Leather Engineering and Technology, University of Dhaka, Dhaka, Bangladesh
*Corresponding author. E-mail: samina@just.edu.bd

ABSTRACT

This study investigated the performance of jute stick charcoal (JSC) as a biosorbent for the removal of hexavalent chromium [Cr(VI)] from an aqueous solution. The batch adsorption experiment was conducted by influencing various experimental conditions like contact time (5–240 min), pH (2–8), initial Cr(VI) concentration (10–100 mg/L), and JSC dose (2–10 g/L). The study result shows that maximum Cr(VI) removal (99%) was found at pH 2, 20 mg/L of initial Cr(VI) concentration, 8 g/L of the JSC dose, and 150 min of equilibrium contact time. Fourier transform infrared (FTIR) spectroscopy and a field emission scanning electron microscope (FE-SEM) were used to characterize the JSC surface characteristics. The Cr(VI) adsorption data of JSC were better described by the Freundlich ($R^2 = 0.995$) and Halsey ($R^2 = 0.995$) isotherm models. The maximum monolayer adsorption capacity of JSC was 11.429 mg/g. Kinetic adsorption data of JSC followed the pseudo-second-order model ($R^2 = 1.0$) as compared with the pseudo-first-order model ($R^2 = 0.97$) and this adsorption process was controlled by chemisorption with multi-step diffusion. Finally, this study revealed JSC as an effective adsorbent for Cr(VI) removal from an aqueous solution.

Key words: adsorption isotherms, adsorption kinetics, chromium(VI), jute stick charcoal

HIGHLIGHTS

- Cr(VI) adsorption was examined using charcoal derived from a jute stick.
- Cr(VI) adsorption onto jute stick charcoal (JSC) increased with an increase in the JSC dose.
- Equilibrium data followed Freundlich and Halsey isotherm models and the highest monolayer adsorption capacity of JSC was found at 11.429 mg/g.
- Kinetic data followed pseudo-second-order kinetic.
- Surface functional groups of JSC influence the Cr(VI) adsorption onto JSC.

GRAPHICAL ABSTRACT

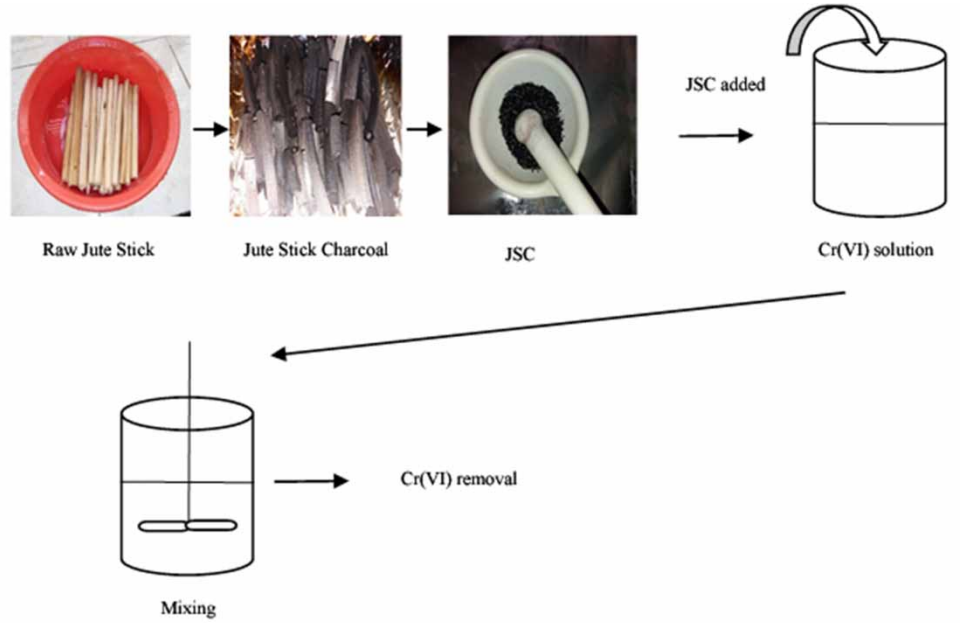

INTRODUCTION

Industrial effluents emit a variety of contaminants, with heavy metals being one of the most serious hazards to the environment. Heavy metals have deadly impacts on flora and fauna when they are above the acceptable limit (Saranya *et al.* 2017). One of the most harmful heavy metals is chromium, which exists in the effluent from industries that use chromium, such as industries involved in leather tanning, electroplating, textile production, and chromium-based product manufacturing (Ghosh *et al.* 2018). When chromium exceeds the allowed limit due to its half-filled electrical form, it is hazardous to the ecology. In aqueous solutions, the two stable forms of Cr are Cr(III) and Cr(VI). (Saranya *et al.* 2018). Cr(VI) is around 300 times more toxic than Cr(III) and because it has high water solubility, it can transport long distances and is highly bioavailable (Ghosh *et al.* 2018). The kidneys, skeletal system, hematological system, and central nervous system in the human body are affected by chromium toxicity (Kaduková & Vircíková 2005). Chromium levels in drinking water should not be more than 0.05 mg/L (WHO 1993). Though industries have treated effluents containing harmful compounds such as Cr(VI), if they exceed permissible levels, they endanger soil, water, air, and ecosystems (Saranya *et al.* 2018). Different methods were used to remove this pollutant from water including ion exchange precipitation, electrocoagulation, adsorption, and reverse osmosis (Khalifa *et al.* 2019) Among heavy metal removal technologies, by far the most versatile and extensively utilized technique is adsorption (Ghosh *et al.* 2018). Over several decades, researchers have employed different biomasses like Date palm empty fruit bunch, Coconut fibers, *Datura stramonium* fruit, *Sargassum horneri* (Torres 2020), rice husk, and rice husk ash (Ghosh *et al.* 2018) for Cr(VI) removal from aqueous solutions using biosorbents. On the contrary, activated carbon or modified activated carbon is considered a possible adsorbent for pollutant removal and is largely used due to its wide surface area, significant porous space, high removal efficiency, different functional groups on the adsorbent surface, fast adsorption kinetics, chemical characteristics, and distinctiveness of regeneration (Ghosh *et al.* 2020). Thus, special high lingocellulosic agro-residues such as jute stick charcoal (JSC) may offer Cr(VI) removal from contaminated water using a readily available, no/low-cost raw material. Jute (*Corchorus olitorius*) is mostly grown in Asian nations such as Bangladesh, India, Bhutan, China, Nepal, and Thailand, and is commonly referred to as the 'golden fiber' (Ray & Ghosh 2018). Jute stick manufacturing on a global scale is predicted to be over 6 million tons annually (Chakraborty *et al.* 2020). Bangladesh is now the world's second-biggest producer of jute. Our nation contributes more than 70%, making it the world's largest exporter of jute fiber (Hossain & Abdulla 2015). Only 4–5 months are needed for jute fiber to grow and create such a large number of ligno-cellulosic sticks (hemicellulose ~30%, cellulose ~41%, lignin ~24%) which composition-wise is equal to woods grown over many years. The jute stick is not good for mulching nor as a feed (Ghosh *et al.* 2019) and as a result, is widely utilized as a source of fuel in

rural areas. In this study, JSC was chosen as an adsorbent due to its availability, cost-effectiveness, and eco-friendly criteria. To the best of our knowledge, there is no study on the removal of Cr(VI) by JSC. Therefore, the objectives of this study are to investigate the applicability of JSC for Cr(VI) removal from aqueous solutions by influencing different experimental parameters like contact time, pH, adsorbent dose, and initial Cr(VI) concentration. Finally, the adsorption behaviors of JSC for Cr(VI) were studied by different kinetics and isotherm models.

MATERIALS AND METHODS

Stock solution preparation

A stock solution of 1,000 mg/L potassium dichromate ($K_2Cr_2O_7$) was made by dissolving potassium dichromate (Grade: ACS reagent, Merck, Germany) in distilled water. A portable digital pH (model pH^{56}, Milwaukce Instruments, Inc., USA) meter was used to determine the pH of the solution. The concentration of the Cr(VI) ion in water was determined using a spectrophotometer (HACH DR, 3900; method 8023) employing the 1,5-diphenylcarbohydrazide technique and a single dry powder formulation termed ChromaVer® 3 chromium reagent for Cr(VI). We determined the total dissolved solids (TDS), electrical conductivity (EC), and salinity using a portable conductivity/TDS meter (sensION $^{+}$EC5, HACH). The applicability of JSC for Cr(VI) removal from tannery effluent was determined using a sample of tannery effluent taken from a tannery in Hazaribagh Tannery Area, Dhaka, Bangladesh.

Biosorbent preparation and characterization

Jute sticks were gathered in the village of Jashore, Bangladesh, then chopped into little pieces (5 inches long). After that, the surface was cleaned with regular tap water and then again with distilled water before being dried at 70 °C in a hot air oven for 48 h to remove any bound substances and pollutants. The dried jute stick was then carbonized for 30 min at 300 °C in a muffle furnace (SXT-10, Shanghai Shuli Instrument and Meters Co., Ltd, China). The carbonaceous jute stick was then cooled, pulverized in a mortar, and sieved to obtain particles with a diameter of 0.5–1.0 mm. Finally, this adsorbent was ready for usage and was packaged in sealed borosilicate glass vials for further investigation. JSC FTIR (Fourier transform infrared spectroscopy) spectra were noted (before Cr(VI) adsorption) using an FTIR-4600 spectrophotometer (JASCO Corporation Ltd, Japan). A field emission scanning electron microscope was used to study the surface morphology of JSC (pre-Cr(VI) adsorption) (FE-SEM, Zeiss Sigma, Carl Zeiss, Germany).

Batch adsorption experiment

Adsorption batch studies were conducted in a 500-mL beaker with a 250-mL working volume solution and adsorbent. During this experiment, 250 mL of a known Cr(VI) solution (made from the stock solution dilution) was added into each beaker and then the pH (with 0.1 M NaOH and 0.1 M HCl) was adjusted, a specified quantity of JSC was added into the solution, a stirring speed of 180 rpm was established and the temperature was maintained at 25 $\pm$ 2 °C. The effects of contact period (5–240 min), pH (2–8), adsorbent dosage (2–10 g/L), and initial Cr(VI) concentration (10–100 mg/L) on Cr(VI) adsorption by JSC were evaluated by utilizing Jar-test equipment (JLT4, VELP Scientifics, Italy) and were performed in duplicate. After concluding the experiment, the adsorbent particle sample was extracted from the beaker using Whatman® glass microfibre filter (grade GF/B) to eliminate adsorbent particles from the solution. The filtrate was further diluted and examined for residual Cr(VI) concentration. The quantity of Cr(VI) adsorbed (q_e) and the removal percentage (R%) of Cr(VI) at the equilibrium stage were estimated by using Equations (1) and (2), respectively:

$$q_e = \frac{(C_o - C_e) \times V}{m} \tag{1}$$

$$R(\%) = \frac{(C_o - C_e)}{C_o} \times 100 \tag{2}$$

where the initial and equilibrium concentrations of Cr(VI) in mg/L are C_o and C_e, respectively. The equilibrium Cr(VI) adsorption in mg/g is given by q_e. The solution volume is V (L), and the adsorbent mass is m (g).

Isotherm experiments

Adsorption of Cr(VI) onto JSC was studied in adsorption isotherm studies at pH 2 with an equilibrium contact period of 150 min, using various concentrations of Cr(VI) (10–100 mg/L) and 8 g/L of fixed adsorbent dose. In this investigation, the operating parameters were identical to batch adsorption studies. The Langmuir, Freundlich, Elovich, and Halsey equilibrium adsorption isotherm models are employed in this investigation. The Langmuir isotherm has been effectively used in heavy metal ion adsorption processes. According to the Langmuir model, monolayer sorption happens on a homogeneous surface with no interaction between adsorbed molecules (Ghosh *et al.* 2018). Equation (3) shows the linear version of the Langmuir (Langmuir 1918) equation in the following:

$$\frac{C_e}{q_e} = \frac{1}{q_{max}b} + \frac{C_e}{q_{max}} \tag{3}$$

where C_e is the remaining Cr(VI) equilibrium concentration in the solution (mg/L), at equilibrium, q_e is the quantity of Cr(VI) adsorbed per mass unit of adsorbent (mg/g), q_{max} is the quantity of Cr(VI) at total monolayer coverage (mg/g), and b (L/mg) is the Langmuir constant linked to adsorption capacity and rate of adsorption. When graphing C_e/q_e vs. C_e, the slope and intercept may be used to calculate the Langmuir parameters. The Langmuir isotherm's most important characteristic is the dimensionless constant separation factor (R_L), which determines whether an adsorption system is 'favorable' or 'unfavorable' (Ngah & Musa 1998). In Equation (4), the separation factor is well-defined as follows:

$$R_L = \frac{1}{1 + bC_0} \tag{4}$$

Unfavorable adsorption is indicated by $R_L > 1$, linear adsorption is indicated by $R_L = 1$, favorable adsorption is indicated by $0 < R_L < 1$, and irreversible adsorption is indicated by $R_L = 0$.

Freundlich's isotherm model is an empirical equation that explains how adsorbent concentration affects the heterogeneous adsorbent surface and adsorption capacity (Dadfarnia *et al.* 2015). The Freundlich isotherm's linearized equation (Freundlich 1906) is presented as the following equation

$$\log q_e = \log K_f + \frac{1}{n}.logC_e \tag{5}$$

where K_f (mg/g) and n are the Freundlich constants and adsorption capacity and intensity, respectively. A linear plot of $logq_e$ vs. $logC_e$ may be used to determine K_f and n. A favorable adsorption process is indicated by n values between 1 and 10, whereas a greater K_f value implies an easier absorption of adsorbate from the solution.

On the kinetic principle, the Elovich model is based, which states that as adsorption occurs, the number of available adsorption sites increases at an exponential rate. This points to a multilayer adsorption mechanism (Ayawei *et al.* 2017). The linearized equation of the Elovich model is expressed in the following equation

$$\ln\frac{q_e}{C_e} = \ln K_e q_m - \frac{q_e}{q_m} \tag{6}$$

where K_e is the Elovich constant and q_m is the Elovich maximum adsorption capacity (mg/g), both of which may be estimated from the slope and intercept of the $ln(q_e/C_e)$ vs. q_e plot.

The Halsey isotherm is a method for determining multilayer adsorption at a distance from the surface (Chakraborty *et al.* 2020). This equation's linearized version is provided in the following equation

$$\log q_e = \frac{1}{n_H}\log K_H - \frac{1}{n_H}.logC_e \tag{7}$$

where the Halsey constants, K_H and n_H, may be found in the intercept and slope of the $logq_e$ vs. $logC_e$ plot, respectively.

Kinetic experiments

For absorption, Cr(VI) kinetic tests were completed at pH 2, 20 mg/L of Cr(VI) solution concentration, and 8 g/L of JSC dosage at 180 rpm at 25 ± 2 °C at various time breaks (5, 10, 15, 30, 60, 90, 120, 150, 180, and 240 min). From the solution mixture, samples were taken and filtered for Cr(VI) analysis. Lagergren's pseudo-first-order model (Lagergren 1898), Ho's pseudo-second-order model (Ho & McKay 1999), intraparticle diffusion model (Weber & Morris 1963), and Boyd model have been used to examine the kinetics of Cr(VI) adsorption. The linearized version of the pseudo-first-order kinetic model equation (Lagergren 1898) is expressed as the following equation

$$\log(q_e - q_t) = \log q_e - \frac{K_1}{2.303}t \tag{8}$$

where q_e represents equilibrium Cr(VI) adsorption in mg/g, at time t, q_t is the amount of Cr(VI) adsorbed (mg/g), and K_1 is the pseudo-first-order rate constant. A linear connection should be seen when plotting $log(q_e - q_t)$ vs. t. K_1 and q_e may be calculated using the plot's slope and intercept.

The adsorption capacity of adsorbate is related to the active sites accessible on the adsorbent surface, rendering to Ho's pseudo-second-order kinetic model (Ho & McKay 1999). Equation (9) shows the pseudo-second-order equation in linear form (with boundary situations $t = 0$ to $t = t$ and $q_t = 0$ to $q_t = q_t$).

$$\frac{t}{q_t} = \frac{1}{K_2 q_e^2} + \frac{1}{q_e}t \tag{9}$$

The initial adsorption rate (h) at $t = 0$ is calculated using the constant K_2, as shown in Equation (10)

$$h = K_2 q_e^2 \tag{10}$$

Replacing the $K_2 q_e^2$ by h in Equation (10), we have Equation (11)

$$\frac{t}{q_t} = \frac{1}{h} + \frac{1}{q_e}t \tag{11}$$

where h is the initial adsorption rate (mg/g/min) and the intercept and slope of a linear plot of t/q_t vs. t provide the constants h and q_e.

Weber and Morris's equation developed the intraparticle diffusion concept (Weber & Morris 1963). Throughout the adsorption process, this model illustrates the existence of intraparticle diffusion. Equation (12) represents the intraparticle diffusion model.

$$q_t = K_{id} t^{0.5} + C \tag{12}$$

K_{id} is the intraparticle diffusion constant rate (mg/g/min$^{0.5}$), which may be calculated using the linear plot slope q_t vs. $t^{0.5}$, and C denotes the plot intercept, it denotes the boundary layer's effect. When the intercept is larger, the rate control step is influenced more by surface adsorption (Wu *et al.* 2005).

The Boyd model was used to further examine the kinetic experimental data to discriminate between the film and pore diffusion steps intricate in the adsorption procedure (Cáceres-Jensen *et al.* 2013). Equation (13) can be used to express the Boyd model:

$$F = \frac{q_t}{q_e} = 1 - \frac{6}{\pi^2}\exp\ (-B_t) \tag{13}$$

where F is the proportion of solute adsorbed at various times t and B_t denotes the function of F. Equation (14) can be used to obtain the B_t value at various contact times, t

$$B_t = -0.4977 - \ln(1 - F) \tag{14}$$

where B_t is calculated for each q_t and then plotted vs. t. Particle diffusion is the rate-limiting phase in the adsorption process if the Boyd linear plot passes through the origin. Otherwise, the rate-limiting stage is film diffusion (Nethaji *et al.* 2013).

RESULTS AND DISCUSSION

Characterization of JSC

The functional properties of JSC were recognized by FTIR analysis (Figure 1). This analysis indicated that there were various functional groups existing on the surface of JSC, which can influence the adsorption process of Cr(VI). Notably, the adsorption peak at 2,987.74 cm^{-1} (C–H stretching vibration of –CH_2–, usually found in hemicellulose, cellulose, and lignin) and 3,608.81 cm^{-1} showed that the existence of bonded O–H groups was the primitive peak of JSC. Carboxylic anhydrides have a C = O stretching vibration, and lactones and ketones were found at 1,734.01 and 1,602.85 cm^{-1}. The peak 1,519.91 cm^{-1} indicates the stretching vibration of amide II. Other peaks at JSC 1,377.17 cm^{-1} (C–N stretching vibration or amine), 1,273.02 cm^{-1} (vibrations of C–O stretching in alcohols), 987.55 cm^{-1} (C = C stretching vibration), 844.82 cm^{-1} (C–H stretching vibration) were observed. Similar types of IR spectrum and functional groups were found by several authors (Chakraborty *et al.* 2020; Ghosh *et al.* 2021a, 2021b). The presence of a porous and uneven surface was indicated by using SEM analysis, which might have played a substantial role in providing high surface area and huge space for active sites (Figure 2).

Effect of contact time and pH on Cr(VI) adsorption

The equilibrium time essential for the biosorption of Cr(VI) onto JSC. The adsorption capabilities of Cr(VI) onto JSC were determined using a contact time range of 5–240 min, as shown in Figure 3(a). The maximum adsorption capacity was 1.53–2.49 mg/g and the removal efficiency was 61–99% (Figure 3(a)). It can be seen that the percent adsorption of Cr(VI) increases with an increase in contact time, reaches equilibrium at about 150 min and then remains constant. Initially, there are many active sites onto the adsorbents and as time progressed, the adsorbate binds with the sites until every site becomes occupied and there is no further adsorption. Ghosh *et al.* (2018) also detected a similar type of Cr(VI) removal from an aqueous solution by rice husk and rice husk ash.

The concentration of hydrogen ions in liquids has an impact on the movement of other ions in an aqueous solution. The effect of pH on metal sorption has been demonstrated in many studies. The rate of Cr(VI) biosorption was primarily influenced by pH, and the study result is presented in Figure 3(b). When the pH of the solution increased from 2 to 8, the Cr(VI) removal by JSC decreased from 99.0 to 4.0%. The Cr(VI) maximum (99%) adsorption was detected at pH 2.0. Protonation causes the biosorbent to be positively charged at low pH

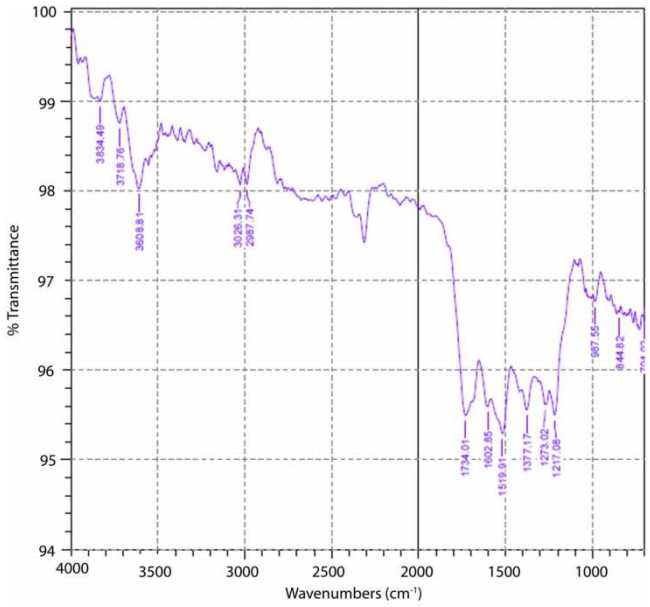

Figure 1 | JSC FTIR spectra before adsorption of Cr(VI).

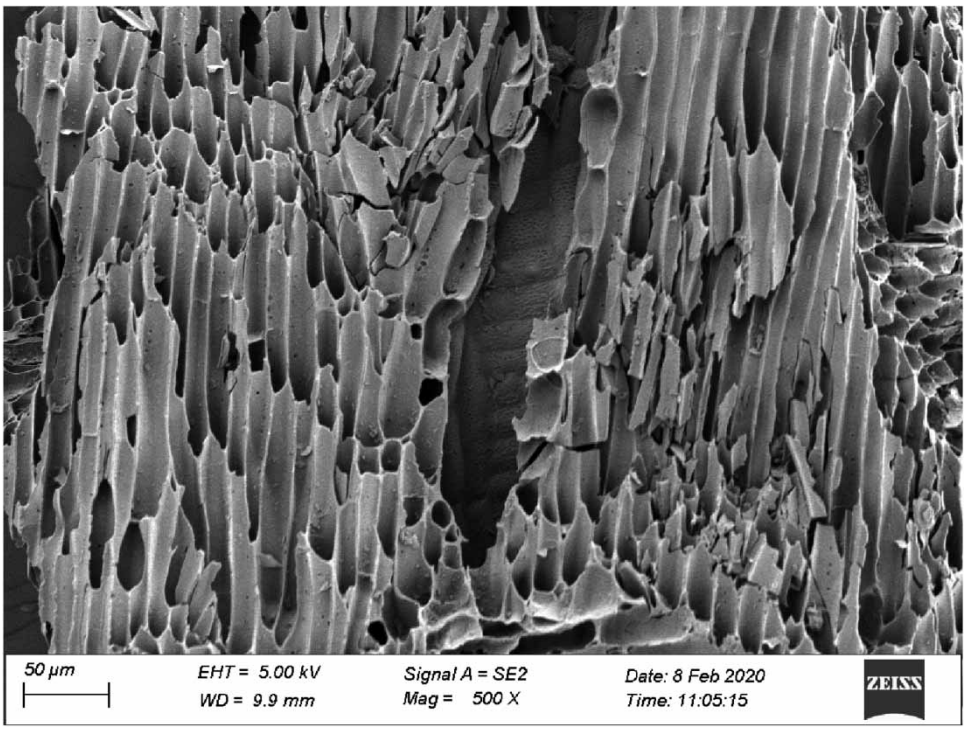

Figure 2 | SEM image of JSC before adsorption of Cr(VI).

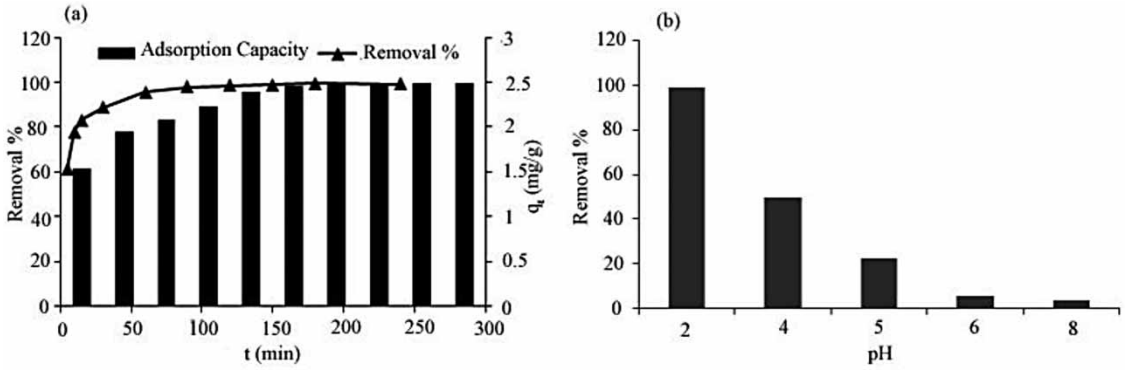

Figure 3 | Effect of (a) contact time and (b) pH on removal of Cr(VI) by JSC (adsorbent dose (8 g/L), rotation speed (180 rpm), initial Cr(VI) concentration (20 mg/L), and temperature (25 ± 2 °C)).

levels. An electrostatic attraction occurs when the dichromate ion functions as the anion (Boddu *et al.* 2003). The adsorption sites are occupied by anionic species, for example, $Cr_2O_7^{2-}$, CrO_4^{2}, $HCrO_4^{-}$, and the reduction in adsorption above pH 4 might be described by the availability of chromium oxyanion and OH^- ions in the bulk (Dönmez & Aksu 2002). Al-Homaidan *et al.* (2018) observed a similar type of result.

Adsorbent dose and initial Cr(VI) concentration effect

The adsorbate adsorption capacity can be measured with the adsorbent dose which is a very important parameter and influenced the removal of contaminants from effluent (Chakraborty *et al.* 2021). The effect of adsorbent JSC dose (2–10 g/L) on the Cr(VI) removal was evaluated at constant contact time (150 min), pH 2, stirring speed (180 rpm), and temperature (25 ± 2 °C) for a fixed 20 mg/L of Cr(VI) concentration. Due to an increase in binding adsorption sites and surface zone, the elimination of Cr(VI) increased from 64 to 99%, when the JSC dosage was raised from 2 to 10 g/L. Adsorption capacity, on the other hand, diminishes with increasing adsorbent dosage (Figure 4(a)), owing to the adsorption site's unsaturation during the adsorption process. As the JSC dosage rose from 2 to 10 g/L, the JSC adsorption capacity for Cr(VI) fell from 6.45 to 2 mg/g. Although there

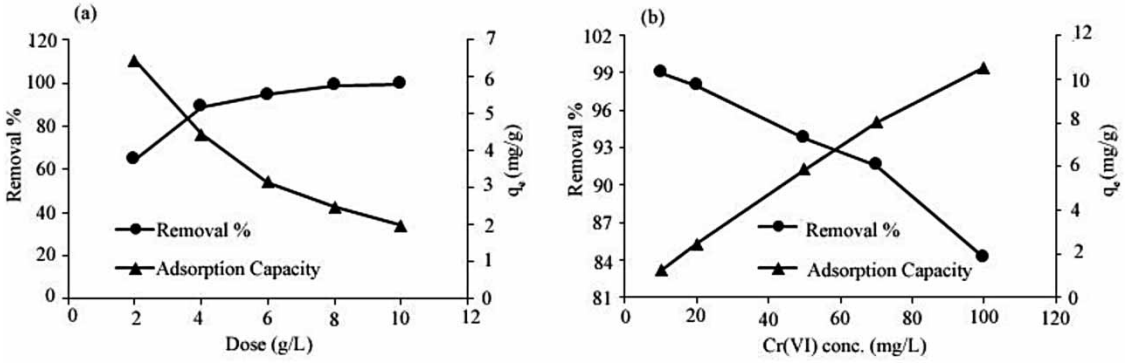

Figure 4 | Effect of (a) adsorbent dose and (b) Cr(VI) initial concentration of Cr(VI) removal by JSC (contact time (150 min), pH (2), temperature (25 ± 2 °C), and rotation speed (180 rpm).

was creation of huge blocks of adsorbent particles at the greatest biomass content; it was possible that this resulted in a decreased surface area accessible for chromium ion sorption (Baral *et al.* 2006).

Figure 4(b) shows that the removal percentage of Cr(VI) decreased (99–84%) with an increasing initial Cr(VI) concentration (10–100 mg/L). The effectiveness of adsorption is determined by two elements. First, when chromium ion concentrations are lower, it provides a positive force that accelerates the adsorption process, and when there are more chromium ions, there is more competition for binding sites in the biomass. Second, when chromium concentrations rise, the proportion of chromium removed decreases. This might be owing to the binding sites becoming saturated (Al-Homaidan *et al.* 2018). On the other hand, JSC adsorption capacity increased (1.24–10.52 mg/g) when the Cr(VI) concentration (10–100 mg/L) increased (Figure 4(b), due to available Cr(VI) ions in aqueous solutions.

Adsorption isotherms

To describe the common behavior between the solutes and the adsorbent, adsorption isotherm is significant. It is also necessary for the design of the adsorption system (Zaman *et al.* 2021). In this study, Langmuir, Freundlich, Halsey, and Elovich models were used to determine the adsorption performance of Cr(VI) onto JSC. They not only give a basic idea of how effective the adsorbents are in removing Cr(VI) but they also describe the maximum quantity of Cr(VI) that the adsorbents can absorb. Figure 5 and Table 1 show the adsorption isotherms and computed values, respectively. The findings showed that the Freundlich ($R^2 = 0.995$) and Halsey ($R^2 = 0.995$) models suited the Cr(VI) adsorption onto JSC better than the Langmuir ($R^2 = 0.982$) and Elovich ($R^2 = 0.974$) models (Table 1). The multilayer adsorption process happens on a heterogeneous surface, according to the Freundlich and Halsey models. This lends credence to the theory that the JSC's surface is made up of tiny heterogeneous adsorption zones that are distinct in terms of adsorption phenomena. Because the value of n (2.327) in the Freundlich isotherm model was greater than 1, JSC was shown to be acceptable for Cr(VI) adsorption from an aqueous solution. The Langmuir model's separation factor values R_L (0.154–0.018) are between 0 and 1, showing that the Cr(VI) adsorption procedure onto the JSC is appropriate, and the higher K_f value (3.499) also suggests that JSC readily uptakes Cr(VI) from the solution (Table 1).

JSC maximal adsorption capacity, according to the Langmuir isotherm, was 11.429 mg/g (Table 1). The Elovich isotherm's reduced adsorption capacity ($q_m = 3.31$ mg/g) and R^2 (0.974) values show that it is unsuitable for explaining the adsorption process of Cr(VI) onto JSC (Figure 5(c)). Table 2 shows JSC's capability for absorption compared to other adsorbents defined in the literature. It indicates that Cr(VI) has a modest maximum monolayer adsorption capacity on JSC and that it is a good alternative adsorbent for the cleaning of heavy metal Cr(VI) from an aqueous solution because of its ease of availability, cheap cost, no secondary contamination, and environmental friendliness.

Adsorption kinetics

Adsorption kinetic studies are significant to determine the efficiency of adsorption and also discover the mechanism and rate-defining step of a chemical reaction. The fitness of experimental data to pseudo-first-order, pseudo-second-order, intraparticle diffusion, and the Boyd model was investigated to explain the adsorption process. All kinetic model parameters and values are shown in Table 3. Based on R^2 value, the pseudo-second-order

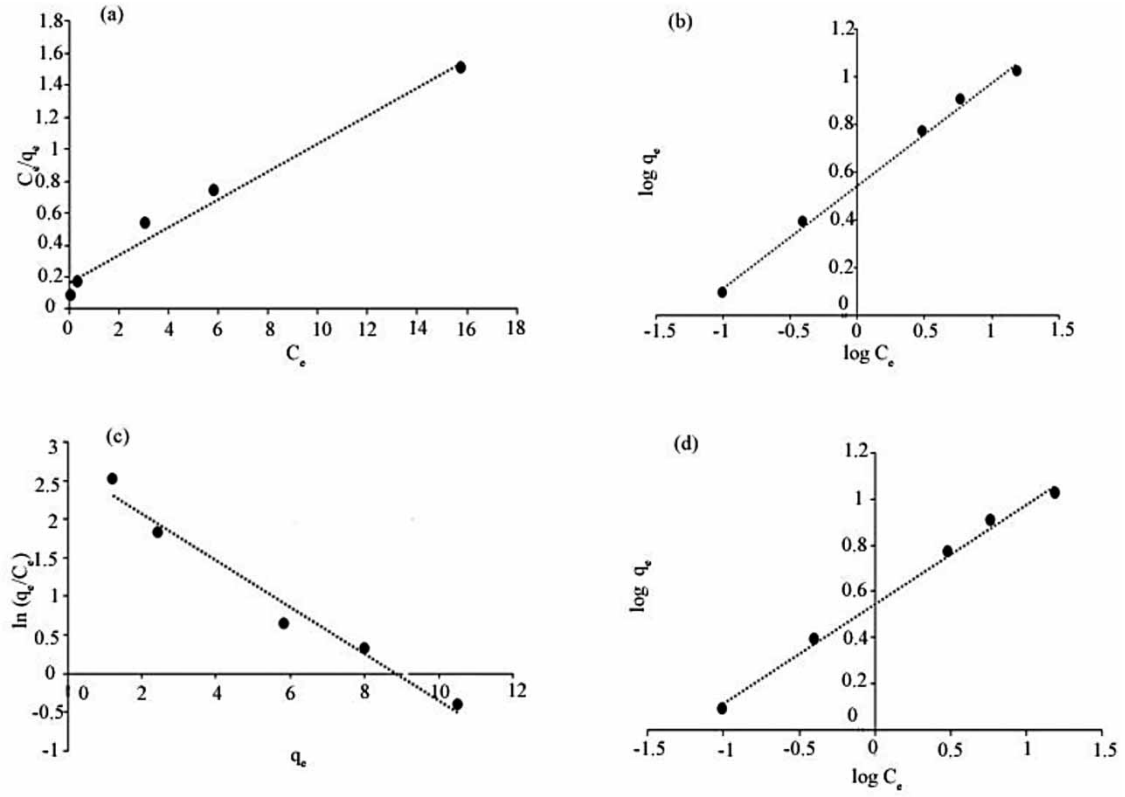

Figure 5 | Adsorption isotherm of Cr(VI) onto JSC using different isotherm models: (a) Langmuir isotherm, (b) Freundlich isotherm, (c) Elovich isotherm, and (d) Halsey isotherm.

Table 1 | Isotherm parameters for Cr(VI) adsorption on JSC

Models	Parameters	Values
Langmuir	q_{max} (mg/g)	11.429
	b (L/mg)	0.550
	R_L	0.154–0.018
	R^2	0.982
Freundlich	K_f (mg/g)	3.499
	n	2.327
	R^2	0.995
Elovich	q_m (mg/g)	3.310
	K_e	2.241
	R^2	0.974
Halsey	n_H	2.327
	K_H	18.45
	R^2	0.995

model (Figure 6(a)) is more close-fitting than the pseudo-first-order model (Figure 6(b)), and for the pseudo-second-order model, the experimental adsorption capacity $q_{e,exp}$. is adjacent to the calculated adsorption capacity $q_{e,cal}$ (Table 3).

So, it is ratified that the sharing or exchange of electrons among Cr(VI) and adsorbent (JSC) and the adsorption process was chemisorption (Bhattacharya & Sharma 2005). The Cr(VI) diffusion process onto JSC was investigated with the intraparticle diffusion model. Throughout the intraparticle diffusion process, metal ions are transferred from solution to the solid phase (Kaya *et al.* 2014). If the data indicate multi-linear plots, the process is divided into two or more parts. Figure 6(c) clearly shows three separate zones: the first linear section (phase I),

Table 2 | Comparison of Cr(VI) adsorption capacity onto JSC with other adsorbents

Adsorbents	Maximum adsorption capacity (mg/g)	pH	References
Magnetic-modified corncob biochar	25.940	3	Van *et al.* (2019)
Paper mill sludge-derived activated carbon	23.180	4	Gorzin & Abadi (2018)
Jute stick charcoal (JSC)	11.429	2	This study
Salix biomass-derived hydrochar	9.760	1	Lei *et al.* (2018)
Freshwater snail shell-derived biosorbent	8.850	2	Zhang *et al.* (2018)
Paper waste sludge derived hydrochar	5.940	3	Nguyen *et al.* (2021)
Rice husk	3.780	2	Ghosh *et al.* (2018)
Rice husk ash	2.270	2	Ghosh *et al.* (2018)

Table 3 | Cr(VI) adsorption's kinetic parameters onto JSC

Models	Parameters	Values
Pseudo-first-order	$q_{e,exp}$, mg/g	2.488
	q_e, mg/g	0.698
	K_1	0.028
	R^2	0.970
Pseudo-second-order	$q_{e,exp}$, mg/g	2.488
	q_e, mg/g	2.531
	K_2	0.117
	h, mg/g/min	0.747
	R^2	1.000
Intraparticle diffusion	K_{id}, mg/g/min$^{0.5}$	0.342–0.011
	C	0.796–2.338
	R^2	0.957–0.9995
Boyd	R^2	0.970

the second linear part (phase II), and lastly the third linear part (phase III). The first linear portion may be responsible for the rapid use of the most readily accessible adsorbing sites onto the adsorbent surface (phase I). The slow diffusion of the adsorbate from the surface area into the interior pores is known as phase II. Finally, phase III is associated with very slow diffusion. Thus, the first component of Cr(VI) adsorption by JSC might be driven by Cr(VI) intraparticle transport exactly by surface diffusion and the latter portion by pore diffusion. On the other hand, the intraparticle diffusion model linear plot did not reach the start, which might be attributable to the difference in mass transfer rates between the start and end phases of adsorption. As a result, the fact that the straight lines from the origin diverge indicates that pore diffusion is not the individual rate-controlling mechanism as shown by the divergence of the straight lines from the origin.

Bhatnagar *et al.* (2010) found similar types of results. The intraparticle diffusion model's linear plot (Figure 6(c)) did not reach the start due to variations in mass transmission from the initial to final stages of the adsorption method, and the intercept (0.796–2.338) value was greater than 0.0, indicating that multiple processes (surface, pore, or firm diffusion) were involved through Cr(VI) adsorption on JSC and that they may have occurred simultaneously (Ghosh *et al.* 2020). The Plot of Boyd kinetic was examined with various contact times of adsorption data to determine the real step through the adsorption procedure. The Boyd plot did not reach the start in Figure 6(d), showing that film diffusion is a part of the adsorption process.

Cr(VI) removal from tannery effluent by JSC

The efficiency of JSC in the Cr(VI) removal from tannery effluent was evaluated after the end of basic adsorption experiments. Tannery effluent sample was collected from Hazaribagh Tannery Area, Dhaka, Bangladesh. At first, the pH, EC, TDS, salinity, and Cr(VI) concentration of sampled wastewater were measured, where values of 2.13, 39.4 ms/cm, 28.5 mg/L, 20.2 g/L, and 9.41 mg/L, respectively, were noted. The pH obtained from basic adsorption experiments was similar to the wastewater, so there was no need to adjust the pH to the removal efficiency

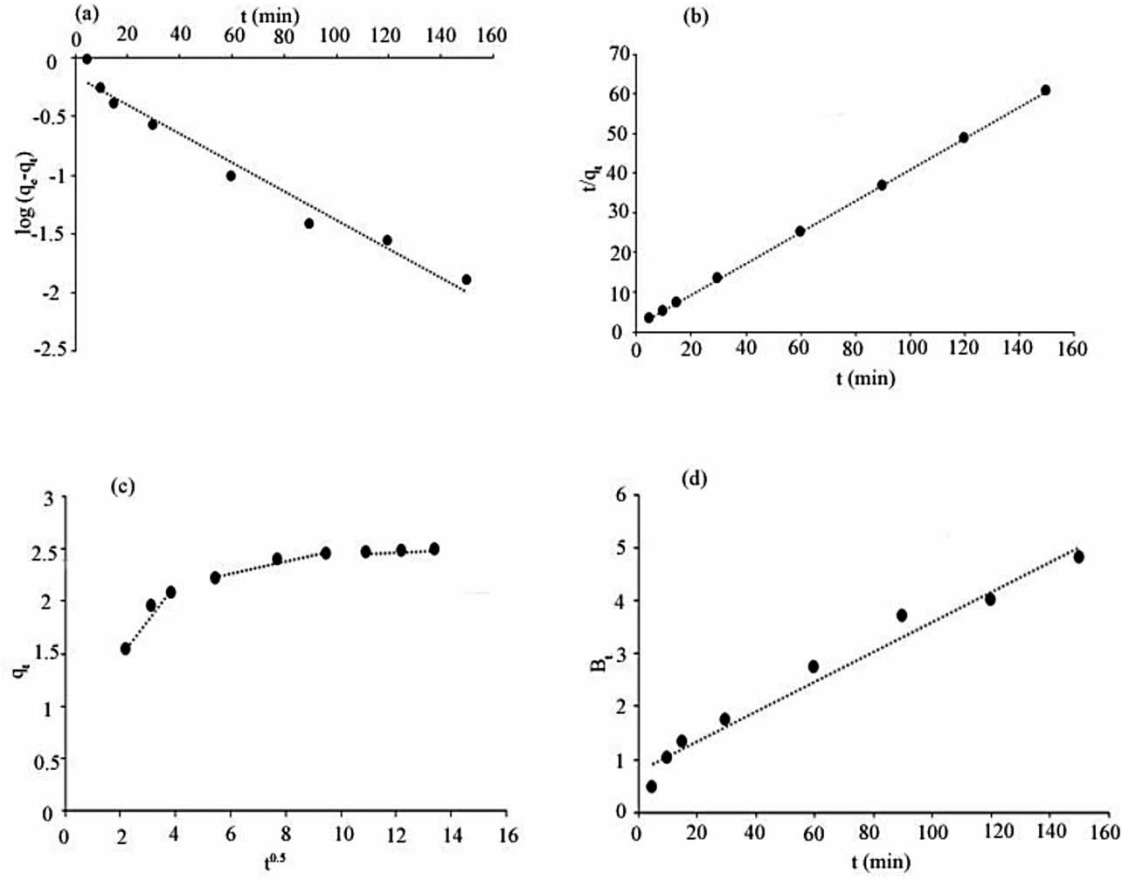

Figure 6 | Cr(VI) adsorption kinetic onto JSC using different kinetic models: (a) pseudo-first-order, (b) pseudo-second-order, (c) intraparticle diffusion and (d) Boyd.

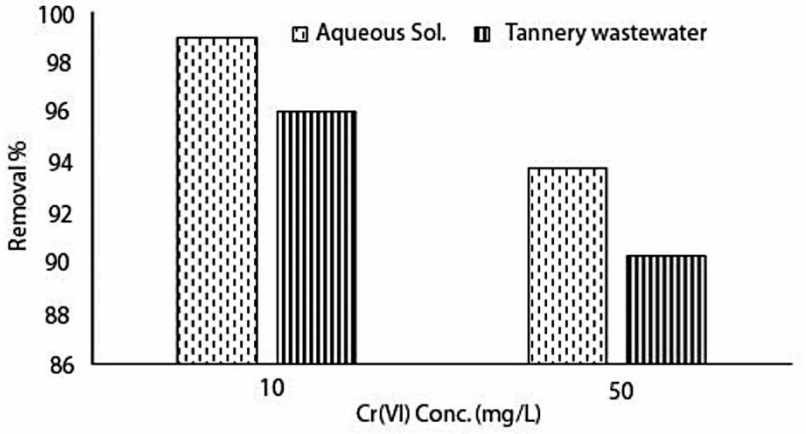

Figure 7 | Cr(VI) removal percentage from an aqueous solution and tannery wastewater.

compared with Cr(VI) aqueous solution as well as real wastewater, the stock solution of Cr(VI) was added into wastewater to obtain desired Cr(VI) concentration (10 and 50 mg/L). Figure 7 illustrates Cr(VI) removal percentage from aqueous solutions and tannery wastewater. When Cr(VI) concentration was 50 and 10 mg/L, the removal percentage was 93.8 and 99% for an aqueous solution and 90.34 and 96.06% for tannery wastewater. This result exposed that the removal efficiency declines with the initial Cr(VI) concentration increase (contact time (150 min), adsorbent dose (8 g/L), temperature (25 $\pm$ 2 °C), and rotation speed (180 rpm). So, JSC is applicable as an effective adsorbent for the removal of Cr(VI) from industrial wastewater.

CONCLUSION

The findings of the current study indicate that the JSC may be effectively utilized as a biosorbent for Cr(VI) removal from aqueous solutions with various controlling parameters like contact time, pH, initial Cr(VI) concentration, and adsorbent dose. The maximum removal was found at pH 2. The Freundlich and Halsey isotherms had a better fit with the experimental data. The highest adsorption capacity of JSC for Cr(VI) removal was found as 11.429 mg/g. Kinetic studies represented that the adsorption process followed the pseudo-second-order kinetic model with multi-steps diffusion process for the adsorption of Cr(VI) on JSC. The FE-SEM and FTIR analyses confirmed that the surface of JSC contains more porous active sites and a variety of functional groups. As a result of its availability, cheap cost, adsorption capacity, and good kinetics, JSC has significant potential for practical use in the adsorptive Cr(VI) removal from an aqueous solution.

ACKNOWLEDGEMENTS

We would like to thank the Department of Environmental Science and Technology, Jashore University of Science and Technology, Bangladesh, for providing the necessary support. We also thank the Ministry of Science and Technology, Bangladesh, for the research grant (R&D) award.

FUNDING

The authors would like to thank the Ministry of Science and Technology, Bangladesh, for the research grant (R&D) award.

DATA AVAILABILITY STATEMENT

All relevant data are included in the paper or its Supplementary Information.

CONFLICT OF INTEREST

The authors declare there is no conflict.

REFERENCES

Al-Homaidan, A. A., Al-Qahtani, H. S., Al-Ghanayem, A. A., Ameen, F. & Ibraheem, I. B. 2018 Potential use of green algae as a biosorbent for hexavalent chromium removal from aqueous solutions. *Saudi Journal of Biological Sciences* **25** (8), 1733–1738. https://doi.org/10.1016/j.sjbs.2018.07.011.

Ayawei, N., Ebelegi, A. N. & Wankasi, D. 2017 Modelling and interpretation of adsorption isotherms. *Journal of Chemistry* **2017**, 1–11. https://doi.org/10.1155/2017/3039817.

Baral, S. S., Das, S. N. & Rath, P. 2006 Hexavalent chromium removal from aqueous solution by adsorption on treated sawdust. *Biochemical Engineering Journal* **31** (3), 216–222. https://doi.org/10.1016/j.bej.2006.08.003.

Bhatnagar, A., Minocha, A. K. & Sillanpää, M. 2010 Adsorptive removal of cobalt from aqueous solution by utilizing lemon peel as biosorbent. *Biochemical Engineering Journal* **48** (2), 181–186. https://doi.org/10.1016/j.bej.2009.10.005.

Bhattacharya, K. G. & Sharma, A. 2005 Kinetics and thermodynamics of methylene blue adsorption on neem (*Azadirachta indica*) leaf powder. *Dyes and Pigmets* **65** (1), 51–59. https://doi.org/10.1016/j.dyepig.2004.06.016.

Boddu, V. M., Abburi, K., Talbott, J. L. & Smith, E. D. 2003 Removal of hexavalent chromium from wastewater using a new composite chitosan biosorbent. *Environmental Science & Technology* **37** (19), 4449–4456. https://doi.org/10.1021/es021013a.

Cáceres-Jensen, L., Rodríguez-Becerra, J., Parra-Rivero, J., Escudey, M., Barrientos, L. & Castro-Castillo, V. 2013 Sorption kinetics of diuron on volcanic ash derived soils. *Journal of Hazardous Materials* **261** (15), 602–613. https://doi.org/10.1016/j.jhazmat.2013.07.073.

Chakraborty, T. K., Islam, M. S., Zaman, S., Kabir, A. H. M. E. & Ghosh, G. C. 2020 Jute (*Corchorus olitorius*) stick charcoal as a low-cost adsorbent for the removal of methylene blue dye from aqueous solution. *SN Applied Sciences* **2** (4), 1–10. https://doi.org/10.1007/s42452-020-2565-y.

Chakraborty, T. K., Ghosh, G. C., Akter, M. N., Adhikary, K., Islam, M. S., Ghosh, P., Zaman, S., Habib, A. & Kabir, A. H. M. E. 2021 Biosorption of reactive red 120 Dye from aqueous solutions by using mahagoni (*Swietenia mahagoni*) wood and bark charcoal: equilibrium, and kinetic studies. *Pollution* **7** (4), 905–921. https://dx.doi.org/10.22059/poll.2021.325135.1110.

Dadfarnia, S., Shabani, A. H., Moradi, S. E. & Emami, S. 2015 Methyl red removal from water by iron based metal-organic frameworks loaded onto iron oxide nanoparticle adsorbent. *Applied Surface Science* **330**, 85–93. https://doi.org/10.1016/j.apsusc.2014.12.196.

Dönmez, G. & Aksu, Z. 2002 Removal of chromium (VI) from saline wastewaters by Dunaliella species. *Process Biochemistry* **38** (5), 751–762. https://doi.org/10.1016/S0032-9592(02)00204-2.

Freundlich, H. M. F. 1906 Over the adsorption in solution. *The Journal of Physical Chemistry* **57**, 385–471.

Ghosh, G. C., Samina, Z. & Chakraborty, T. K. 2018 Adsorptive removal of Cr(VI) from aqueous solution using rice husk and rice husk ash. *Desalination and Water Treatment* **130**, 151–160. https://dx.doi.org/10.5004/dwt.2018.22828.

Ghosh, R. K., Ray, D. P., Debnath, S., Tewari, A. & Das, I. 2019 Optimization of process parameters for methylene blue removal by jute stick using response surface methodology. *Environmental Progress & Sustainable Energy* **38** (5), 13146. https://doi.org/10.1002/ep.13146.

Ghosh, G. C., Chakraborty, T. K., Zaman, S., Nahar, M. N. & Kabir, A. H. M. E. 2020 Removal of methyl orange dye from aqueous solution by a low-cost activated carbon prepared from mahagoni (*Swietenia mahagoni*) bark. *Pollution* **6** (1), 171–184. https://dx.doi.org/10.22059/poll.2019.289061.679.

Ghosh, R. K., Ray, D. P., Chakraborty, S., Saha, B., Manna, K., Tewari, A. & Sarkar, S. 2021a Cadmium removal from aqueous medium by jute stick activated carbon using response surface methodology: factor optimisation, equilibrium, and regeneration. *International Journal of Environmental Analytical Chemistry* **101** (14), 2171–2188. https://doi.org/10.1080/03067319.2019.1700964.

Ghosh, R. K., Ray, D. P., Tewari, A. & Das, I. 2021b Removal of textile dyes from water by jute stick activated carbon: process optimization and isotherm studies. *International Journal of Environmental Science and Technology* **18** (9), 2747–2764. https://doi.org/10.1007/s13762-020-03003-5.

Gorzin, F. & Abadi, M. M. B. R. 2018 Adsorption of Cr(VI) from aqueous solution by adsorbent prepared from paper mill sludge: kinetics and thermodynamics studies. *Adsorption Science & Technology* **36** (1–2), 149–169. https://doi.org/10.1177/0263617416686976.

Ho, Y. S. & McKay, G. 1999 Pseudo-second order model for sorption processes. *Process Biochemistry* **34** (5), 451–465. https://doi.org/10.1016/S0032-9592(98)00112-5.

Hossain, M. M. & Abdulla, F. 2015 Jute production in Bangladesh: a time series analysis. *Journal of Mathematics and Statistics* **11** (3), 93–98. https://doi.org/10.3844/jmssp.2015.93.98.

Kaduková, J. & Vircíková, E. 2005 Comparison of differences between copper bioaccumulation and biosorption. *Environmental International* **31** (2), 227–232. https://doi.org/10.1016/j.envint.2004.09.020.

Kaya, K., Pehilivan, E., Schmidt, C. & Bahadir, M. 2014 Use of modified wheat bran for the removal of chromium(VI) from aqueous solutions. *Food Chemistry* **158**, 112–117. https://doi.org/10.1016/j.foodchem.2014.02.107.

Khalifa, E. B., Rzig, B., Chakroun, R., Nouagui, H. & Hamrouni, B. 2019 Application of response surface methodology for chromium removal by adsorption on low-cost biosorbent. *Chemometrics and Intelligent Laboratory Systems* **189**, 18–26. https://doi.org/10.1016/j.chemolab.2019.03.014.

Lagergren, S. 1898 Zur theorie der sogenannten adsorption geloster stoffe. *Kungliga Svenska Vetenskapsakademiens Handlingar* **24** (4), 1–39.

Langmuir, I. 1918 The adsorption of gases on plane surfaces of glass, mica and platinum. *Journal of the American Chemical Society* **40** (9), 1361–1403. https://doi.org/10.1021/ja02242a004.

Lei, Y., Su, H. & Tian, F. 2018 A novel nitrogen enriched hydrochar adsorbents derived from salix biomass for Cr(VI) adsorption. *Scientific Reports* **8** (1), 1–9. https://doi.org/10.1038/s41598-018-21238-8.

Nethaji, S., Sivasamy, A. & Mandal, A. B. 2013 Adsorption isotherms, kinetics and mechanism for the adsorption of cationic and anionic dyes onto carbonaceous particles prepared from Juglans regia shell biomass. *International Journal of Environmental Science and Technology* **10** (2), 231–242. https://doi.org/10.1007/s13762-012-0112-0.

Ngah, W. W. & Musa, A. 1998 Adsorption of humic acid onto chitin and chitosan. *Journal of Applied Polymer Science* **69** (12), 2305–2310. https://doi.org/10.1002/(SICI)1097-4628(19980919)69:12<2305::AID-APP1 > 3.0.CO;2-C.

Nguyen, L. H., Van, H. T., Nguyen, Q. T., Nguyen, T. H., Nguyen, T. B. L., Nguyen, V. Q., Bui, T. U. & Sy, H. L. 2021 Paper waste sludge derived-hydrochar modified by iron (III) chloride for effective removal of Cr(VI) from aqueous solution: kinetic and isotherm studies. *Journal of Water Process Engineering* **39**, 101877. https://doi.rg/10.1016/j.jwpe.2020.101877.

Ray, D. P. & Ghosh, R. K. 2018 Perspective of jute in a new realm beyond sacking. *Economic Affairs* **63** (4), 981–986. https://doi.org/10.30954/0424-2513.4.2018.22.

Saranya, N., Nakkeeran, E., Shrihari, S. & Selvaraju, N. 2017 Equilibrium and kinetic studies of hexavalent chromium removal using a novel biosorbent: Ruellia Patula Jacq. *Arabian Journal for Science and Engineering* **42** (4), 1545–1557. https://doi.org/10.1007/s13369-017-2416-3.

Saranya, N., Ajmani, A., Sivasubramanian, V. & Selvaraju, N. 2018 Hexavalent Chromium removal from simulated and real effluents using Artocarpus heterophyllus peel biosorbent-Batch and continuous studies. *Journal of Molecular Liquids* **265**, 779–790. https://doi.org/10.1016/j.molliq.2018.06.094.

Torres, E. 2020 Biosorption: a review of the latest advances. *Processes* **8** (12), 1–23. https://doi.org/10.3390/pr8121584.

Van, H. T., Nguyen, L. H., Mac, D. H., Vu, T. T., Hoang, L. P. & Nguyen, X. C. 2019 Removal of Cr(VI) from aqueous solution using magnetic modified biochar derived from raw corncob. *New Journal of Chemistry* **43** (47), 18663–18672. https://doi.org/10.1039/C9NJ02661D.

Weber, W. J. & Morris, J. C. 1963 Kinetics of adsorption on carbon from solution. *Journal of the Sanitary Engineering Division* **89** (2), 31–59. https://doi.org/10.1061/JSEDAI.0000430.

World Health Organization 1993 *Guidelines for Drinking-Water Quality*. World Health Organization, Geneva.

Wu, R., Qu, J. & Chen, Y. 2005 Magnetic powder MnO-Fe_2O_3 composite-a novel material for the removal of azo-dye from water. *Water Research* **39** (4), 630–638. https://doi.org/10.1016/j.watres.2004.11.005.

Zaman, S., Mehrab, M. N., Islam, M. S., Ghosh, G. C. & Chakraborty, T. K. 2021 Hen feather: a bio-waste material for adsorptive removal of methyl red dye from aqueous solutions. *H_2Open Journal* **4** (1), 291–301. https://doi.org/10.2166/h2oj.2021.123.

Zhang, X., Lv, L., Qin, Y., Xu, M., Jia, X. & Chen, Z. 2018 Removal of aqueous Cr(VI) by a magnetic biochar derived from Melia azedarach wood. *Bioresource Technology* **256**, 1–10. https://doi.org/10.1016/j.biortech.2018.01.145.

First received 22 June 2022; accepted in revised form 4 October 2022. Available online 18 October 2022